Prediction of Seizure Spread Network via Sparse Representations of Overcomplete Dictionaries

Feng Liu[1], Wei Xiang[2], Shouyi Wang[1], and Bradley Lega[3]

[1] Department of Industrial, Manufacturing & Systems Engineering,
[2] Department of Computer Science and Engineering,
University of Texas at Arlington,
Arlington, TX 76019, USA
feng.liu@mavs.uta.edu, wei.xiang@mavs.uta.edu, shouyiw@uta.edu,
[3] Neurological Surgery, University of Texas Southwestern,
Dallas, TX 75253, USA
bradley.lega@utsouthwestern.edu

Abstract. Epilepsy is one of the most common brain disorders and affect people of all ages. Resective surgery is currently the most effective overall treatment for patients whose seizures cannot be controlled by medications. Seizure spread network with secondary epileptogenesis are thought to be responsible for a substantial portion of surgical failures. However, there is still considerable risk of surgical failures for lacking of priori knowledge. Cortico-cortical evoked potentials (CCEP) offer the possibility of understanding connectivity within seizure spread networks to know how seizure evolves in the brain as it measures directly the intracranial electric signals. This study is one of the first works to investigate effective seizure spread network modeling using CCEP signals. The previous unsupervised brain network connectivity problem was converted into a classical supervised sparse representation problem for the first time. In particular, we developed an effective network modeling framework using sparse representation of over-determined features extracted from extensively designed experiments to predict real seizure spread network for each individual patient. The experimental results on five patients achieved prediction accuracy of about 70%, which indicates that it is possible to predict seizure spread network from stimulated CCEP networks. The developed CCEP signal analysis and network modeling approaches are promising to understand network mechanisms of epileptogenesis and have a potential to render clinicians better epilepsy surgical decisions in the future.

Keywords: Brain connectivity, Sparse representation, Feature selection, CCEP, Seizure spread network

1 Introduction

The human brain is among the most complex systems known to mankind [2]. There has been a great deal of neurophysiological researching attempting to understand brain functions and networks through detailed analysis of neuronal excitability and synaptic transmission [9][10]. Though the advances in brain imaging techniques have enabled many studies to investigate brain functional connectivity with widely variable spatial and temporal resolution using different neurophysiology and neuroimaging modalities including electroencephalography (EEG), magnetoencephalography (MEG), functional near-infrared spectroscopy (fNIRS), and functional MRI (fMRI) approaches [16][20]. However, most of current work on brain functional connectivity analyzes at a relatively coarse level of connectivity of the intrinsic dynamic brain network. The results

are often at odds with the longstanding neuroscientific theory[7]. In this paper, we employ cortico-cortical evoked potentials (CCEPs) which directly measure the local neural activity inside brain to map effective brain connectivity via stimulation. The major advantage of mapping brain connectivity via stimulation is the ability to assess directed dynamical spread networks and discover functional cortical connections in vivo, which is not possible using MRI-based tract tracing nor with the fMRI-based covariance methods [6].

To understand pathology of epilepsy, more researchers are focusing on abnormal brain network connectivity. Historically speaking, there are two opposing perspective to view brain functionality: integration and segregation. The former views different areas of cortex collaborate together to perform certain tasks, such as attention, memory processing, etc. However the latter perspective think the "segregated" area of cortex is responsible for certain functionality of the brain, such as language, emotion etc. A good discussion of integration and segregation can be found in the Nature Review paper[3]. The advantage of the former one is to investigate brain in a more systematic view by searching distinction of functional and effective connectivity among patients and controls. Moreover, the emerging interdisciplinary area of complex network theory can offer a systematic measurement of network characteristics with great capability to model networks in nature and man-made complex systems[26][1][19][8]. Recently, an increasing number of theoretical and empirical studies approach the function of the human brain from a network perspective, i.e., the integration paradigm. The aim of human connectomics is to uncover the underlying dynamics associated with their connectivity. Disturbed interaction among brain areas is associated with brain and mental disorder [21][22]. Many researchers have verified that a large amount of brain diseases arise from dysfunction of brain network [28][30] [24]. CCEP offers the possibility of understanding effective connectivity within seizure networks to improve diagnosis and identify resection candidates for seizure surgery to a finer spatial resolution. In our paper, CCEP signals are used to construct connectivity of epilepsy patients in order to predict the ictal onset spreading network. The rest of paper is organized as follows: data description and preprocessing is presented in Section 2; The presented supervised sparse feature selection formulation is given in Section 3. The experimental result of spread network prediction is given in Section 4; Section 5 concludes this paper and future research is also described.

2 Data Processing and Visualization

2.1 Data Acquisition

Patients were drawn from the surgical epilepsy program at University of Texas Southwestern Medical Center (UTSW), the preeminent surgical epilepsy program in a metropolitan area of 7 million people. We have also analyzed subset of our existing database of intracranial electrode implantations [15] (as described in Table. 1) that have both structural MRI and CCEP mapping. Prior to electrode implantation, patients undergo resting-state fMRI as well as detailed structural MRI including diffusion-tensor imaging (DTI).

2.2 Stimulation Polarity

Stimulations (conducted using the Grass S88 stimulator (Warwick, RI, USA) [15]) show switched polarity pattern due to the bipolar stimulation was applied between adjacent electrodes by switching anode and cathode electrodes. The reason we prefer bipolar stimulation as opposed to unipolar stimulation where the stimulation is performed

Subject ID	Sex	Age	Duration (years)	Total seizures	Early spread	Late spread	Seizure analyzed	Onset pattern	Onset site	Early site	Late site
1	M	59	8	4	0.2	30	4	4	R entorhinal	MTG	Insula
2	F	38	8	7	2	13	5	4	R amygdala	Para hippocampu	STG
3	M	30	21	3	0.3	12	3	1	L precuneus	Fusiform	Lingula
4	F	63	54	14	0.3	9	5	4	L angular g.	MTG	Fusiform
5	F	42	15	5	0.6	10	5	4	R planum polare	STG	Supramarginal

Table 1: Information of 5 patients studied in this paper, who undergo the surgical epilepsy program at UTSW.

between an area of interest and a distant site, is that bipolar stimulation allows for more localized current flow in the cortex beneath electrodes, thereby minimizing the spatial spread of stimulation and increasing its spatial resolution [12][18]. In this paper, we show that stimulation responses categorized based on polarity of stimulus are related to the CCEPs measured and thereof we suggest to divide signals into groups based on polarity of stimulus and then choose those from positive and negative group separately for further analysis, as explained later.

In most studies [11] CCEPs at each site were averaged before any task of data mining to be done, however, in this paper we separate them out and term the responses resulted from stimulus showing positive polarity as the *Positive Group*, and that from stimulus of negative polarity as the *Negative Group*. For comparison, we also average all CCEPs despite of its source and name it as the *Mixed Group*. In this paper, we refer to the averaged response from three different groups using positive/negative/mixing averaged response. Fig. 1 illustrates two examples of the comparison between responses from three groups.

It is worth noting that in Fig. 1(a), the positive and negative averaged response demonstrate a *semi*-symmetrical structure where the momentum on the first 80ms is affected by a dynamic force. We believe such dynamics were caused by neuronal activities of those attempting to recover to its normal state. Besides, some averaged responses like Fig. 1(b) can be treated as irregular ones since positive and negative averaged responses do not follow a similar trend (i.e. increase/decrease at different phases).

With both groups, it is not wise to average signals over all trials (i.e., analyzing on the black dotted signals shown in Fig. 1). The underlying tissue (which may be more sensitive to one polarity) will show averaged response in one group that have larger amplitude at all phases comparing to the other's. If we compare mixing averaged response with either positive or negative one, most likely we will see some prominent features weakened due to a distinguishable profile of the averaged response signal, including 1) semi-symmetry and 2) sensitivity to different polarity of stimulus. Therefore, we need to extract signals whose averaged response is stronger with respect to the polarity of its source of stimulus.

2.3 Data Preprocessing

In this paper, to simplify further data analysis using averaged signals, we extract and only work with the positive group (exemplified by Fig. 3). To remove post-stimulation artifacts which occur nondeterminately at various times between 85ms to 95ms, peak and valley detection algorithm is applied following which we retrieve signals from +1ms till +900ms (for some sites, there exist strong response immediately after the timing of post-stimulation artifact). After that, Savitzky-Golay filter is applied to smooth all signals without greatly distorting the signals. Many of stimulus signals jitter with sine

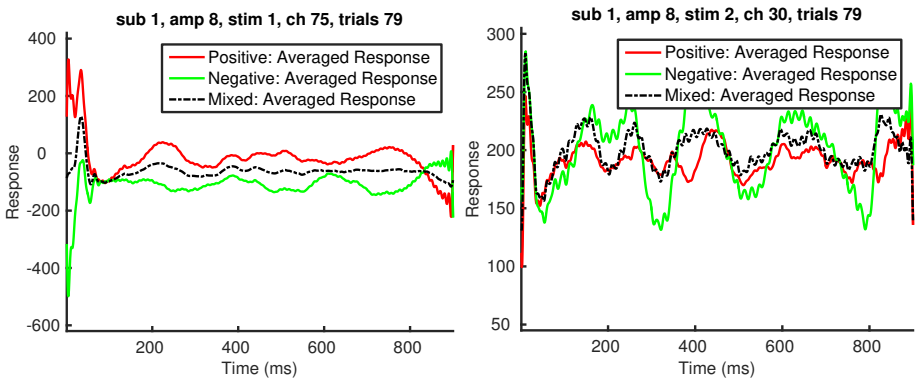

(a) A typical semi-symmetrical example (b) An irregular example

Fig. 1: Comparison of positive, negative and mixing averaged signals categorized according to the polarity of stimulus signals. Most paper studied on signals drawn with the black dotted line while in this paper, we think polarity factor should be taken into account when doing further data analysis.

waves whose frequency is found fixed at 49Hz. To alleviate this problem, we apply a specific designed band-pass filter to attenuate artifact-induced frequency at 49Hz, as well as those frequencies from 1 to 3Hz and outside 100Hz. Besides, by analyzing patterns of the stimulus signals, we find it necessary to remove outlier trials as they give rise to much stronger and longer CCEPs. To this end, all trials were further taken care of statistically using the approach of trimmed mean, i.e. for all trials stimulated on the same pair of sites, we remove those generated from stimulus signals whose trimmed means are two standard deviations away from mean of the distribution of trimmed means over all stimulus signals at the two stimulation sites (with 25 percent of the ends discarded). This guarantees all trials are generated from similar stimulations. Afterwards. trimmed mean approach is also used for every channel in order to get rid of outlier trials. Take for example subject **1**: during four stimulations with amplitude 8mA on CP1-CP2, UP2-UP3, UP5-UP6 and UP7-UP8 respectively, there are 80 trials among all the 140 channels. Trimmed mean approach based on stimulus signals helps get rid of 10, 13, 9, 10 trials for each of the four stimulations respectively, while the trimmed mean approach based on channels removes 2 trials per channel. The signal responses over all trials on one channel can be visualized using event-related potential (ERP) plot [4], by which the visualization of expected stimulation along trials should have a clear curve belonging to similar colormap (shown in Fig. 2). Finally, we convert signals to Z-scores so that for most signals their strengths are fixed from -5 to +5 as in Fig. 3.

3 Supervised Sparse Feature Selection

3.1 Experimental Design of features

When it comes to modeling the brain connectivity based on the measurement of how similar two channels' time series signals are, there are many options to be chosen. The most popular ones can be categorized as linear and nonlinear measurements [14][23], linear ones include cross correlation, coherence,and nonlinear measurements include mutual information, transfer entropy, Granger causality, phase synchronization, etc.

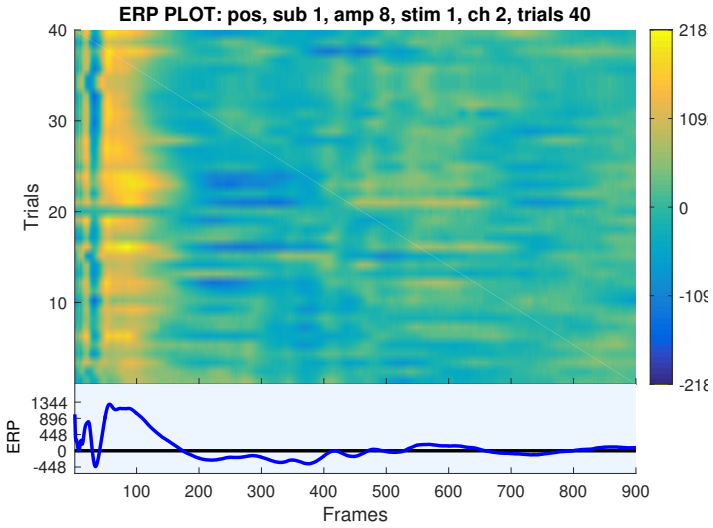

Fig. 2: An example of ERP plot, where the signal responses can be visualized clearly with similar colormap along trials.

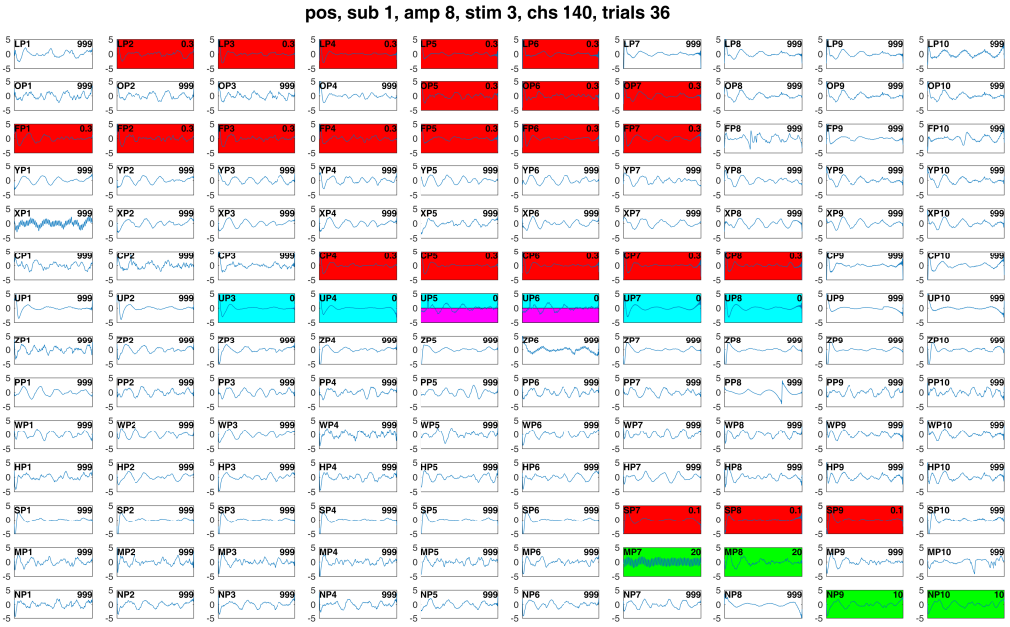

Fig. 3: Normalized Z-scores from positive averaged responses on 140 channels for patient 1. The signals were averaged over 36 repetitive 8mA stimulations on channel UP3 and UP4. Magenta colored regions indicate stimulus sites, cyan indicates seizure onset zone, and red and green indicate EARLY and LATE ictal spread respectively[15]. For e.g., UP5, UP6 are both stimulus site and seizure onset zone.

Different measurement will usually result in different networks, combined with the lack of ground truth information, it's hard to determine which one is more reasonable and accurate. However our case is different since we have a supervised label that was generated from the spread network, which makes it possible to compare prediction accu-

racy from different methodologies. The other choices come from the data preprocessing step and an appropriate frequency band need to be selected, the band pass filter level includes . Moreover, according to our analysis, we want to explore the effected network from both positive stimulus and negative stimulus, we also want make a contrast without considering the positive and negative stimulus. Another experimental design consideration includes the epoch signal length after the stimulus, we assume that after the stimulus, there is a transient period and it's hard to measure that exact length since every channel exhibits different temporal behavior. We picked 0.3s, 0.5s, 0.7s and 0.8s as different levels of the time series length. Other options is that we have different stimulus amplitude, which are 2 mA, 4 mA, 6 mA and 8 mA. All those different type of choices are different factors in the perspective of experimental design, they all have different levels. Another antagonistic choices comes when aggregating across different trials under the same conditions, as the impulsive stimulus signals were applied to the same channel about 40 times under the condition of the same stimulus amplitude, the same stimulus sites for the same person. One way of aggregation is to calculate the averaged epoch time series first and then calculate the adjacency matrix using different similarity measurement. The advantage of average first is to eliminate white noise in the channels, however the disadvantage is that more precise connectivity information at different time period might be lost. The opposing paradigm is to calculate the neural synchrony similarity measurement first and then aggregate on the adjacency matrix, we try to use both ways to predict the spread network. We call those two options trial aggregation design.

To sum up, we did a comprehensive full factorial design of experiment with 6 factors, including (1) similarity measurements, (2) positive, negative vs overall stimulus, (3) stimulus amplitude, (4) epoch signal length following stimulus, (5) frequency band-pass design, (6) trial aggregation design. The frequency band-pass have 6 levels, which are 4-100 Hz, 4-8 Hz, 8-13 Hz, 13-25 Hz, 25-40 Hz, 30-100 Hz; the neural time series similarity measurements used in our research include cross correlation, coherence, mutual information, transfer entropy, phase synchronization and dynamic time warping. In table 2, a summary of level counts for each factor is given.

factor	**number of levels**
similarity measurements	6
positive, negative vs overall stimulus	3
stimulus magnitude	4
epoch signal length	4
band pass frequency	6
trial aggregation design	2

Table 2: Number of levels of different factors. The number of features here in our exploration is the number of full factorial of all the six factors in our design, which is 3456 features.

3.2 Sparse Feature Selection

In order to select the most useful features, we used a sparse feature selection method procedure regularized with L_1 norm. The idea behind of the sparse representation is that we want to represent connection vector y as a linear combination of the fewest features from the overcomplete dictionary [27], which becomes a powerful tool for biomedical data [29]. Here we use a sparse feature selection model which allows certain degree of noise, and the goal function is given below:

$$J_1(x;\lambda) = \|y - Ax\|_2^2 + \lambda\|x\|_1 \tag{1}$$

where $A \in R^{n \times k}$ is the overcomplete dictionary with each column being the prediction results using our factorial experimental design of 6 factors, n is the number of nodes and k is the number of features, $y \in R^n$ is the supervised connection vector. The first part of Eq.(1) is to measure the sparse representation error and the second term is trying to make the selected features to be sparse compared to the over-complete dictionary. By minimizing the goal function, we will get the selected ensemble of prediction methodologies. Unlike the traditional ensemble method [25], our learned vector x signifies the supervised weighted version of an ensemble of weak classifiers. As a result, our problem becomes a classic ℓ_1-penalized least-squares problem. There are plenty of algorithms to solve it available [17] [27] [5], here in our research, we use Homotopy algorithm proposed in [5]. For more detailed description of Homotopy algorithm, please refer to Donoho and Tsaig's paper [5].

4 Network Connectivity Modeling and Prediction

4.1 Spread Network Construction and Prediction

Like our previous work [15], in this paper we refined CCEP paradigm to analyze the seizure spread from ictal onset zones to EARLY and LATE sites of seizure propagation, defined as spread from onset site before or after 3s.

By better understanding the epilepsy ictal onset spread network, we can resect pathological path and reduce the potential destruction of functionality in other cortical region. Promising clinical results from [13] show that 42% of patient are seizure free after resective epilepsy surgery based on seizure ictal onset spreading network.

In every similarity measurement, it's nontrivial to select the threshold to get the connected network with appropriate density. Take the calculation of cross correlation for each trial as an example, we observed a time variant adjacency matrix. If the same threshold is used, sometime, a very densely connected network is generated, for another stimulus trial, a very sparsely connected network is generated. Furthermore, we observed that if we average time series from all epoch trials first and then compute the cross correlation, the resulting correlation coefficients are much higher than directly calculating correlation for each trial. To solve that problem, a dynamically adjusted threshold is used in the paper. The dynamically adjusted threshold is based on the priori knowledge of average degree on brain network, which has been extensively studies in the literature.

The predesignated percentage is calculated based on the following equation:

$$p = \frac{k}{(N-1)} * 100\% \tag{2}$$

Using p to get the percentile in the correlation matrix, we can generate a network with the average degree to be k.

4.2 Experimental Result

Based on the framework mentioned, We conducted the sparse feature selection of the first two patients' seizure onset spreading network, and test the learned features on the next three patients and achieved 72.3% accuracy. Since we have 6 factors, it's impossible to give a comprehensive accuracy result. We illustrate 2 factors, namely, the similarity measurements and band pass frequency design in the following table. The training accuracy is 80.5% and the testing accuracy is 72.3%. Generally speaking, the correlation and mutual information measurement perform better than the other 4 measurements.

	Training						Testing					
	Corr	Cohe	MI	TE	PS	DTW	Corr	Cohe	MI	TE	PS	DTW
4-100Hz	72.3%	69.3%	74.3%	73.5%	68.8%	62.3%	71.3%	68.6%	74.6%	72.7%	68.4%	60.8%
4-8Hz	68.7%	66.1%	67.4%	70.2%	69.2%	59.3%	66.6%	67.5%	68.2%	68.8%	70.0%	61.2%
8-13Hz	65.2%	54.0%	68.3%	64.2%	67.3%	61.8%	65.9%	63.0%	68.1%	63.4%	64.7%	62.1%
13-25Hz	71.4%	67.4%	69.7%	69.0%	66.2%	63.0%	69.9%	66.6%	68.8%	70.2%	65.9%	63.4%
25-40Hz	70.5%	69.3%	70.2%	71.1%	65.4%	65.9%	71.4%	67.9%	70.3%	72.1%	65.2%	72.0%
30-100Hz	71.8%	72.5%	73.9%	68.5%	71.7%	64.8%	71.1%	71.5%	74.5%	68.3%	71.9%	63.9%
Sparse	80.5%						72.3%					

Table 3: Accuracy Summary. Abbreviations– Corr: Correlation, Cohe: coherence, MI: mutual information, TE: transfer entropy, PS: phase synchronization, DTW: dynamic time warping.

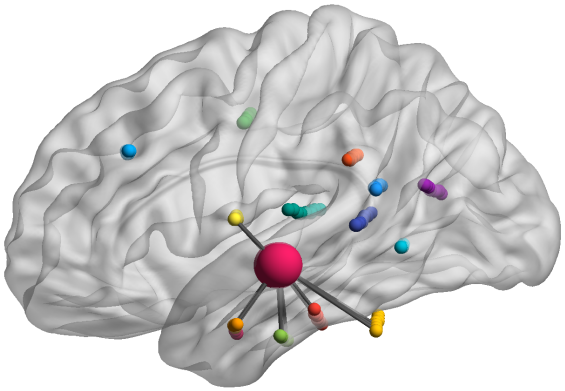

Fig. 4: Spread network of Patient 1: the large red node is the seizure onset area, and the connected nodes to the large red node are the cortical sites where seizure arrives within 3s.

Take patient 1 as an illustrative example, the predicted spread network is given in Fig.5 compared to Fig.4, which is the real seizure spread network. To the best of our knowledge, we are among the first to investigate prediction of seizure spread network using using CCEP singals processing and data mining analytic approaches. The prediction accuracy of more than 70% achieved in this preliminary study is promising to confirm that it is possible to predict fast seizure spread locations from CCEP signals. Such information will be of great importance for neurosurgeons to make better surgery plan and improve success rate for patients with epilepsy.

5 Conclusion

In this paper, we proposed to predict seizure ictal onset spread network which is a missing part in literature. In our work, we implemented an extensive experimental design using 6 factors. We separately investigated both positive and negative stimulated signals, thus giving us additional information when extracting features. A sparse learning framework of over complete dictionary is presented, the framework is scalable that more effecting factors can be added. We converted unsupervised brain network connectivity

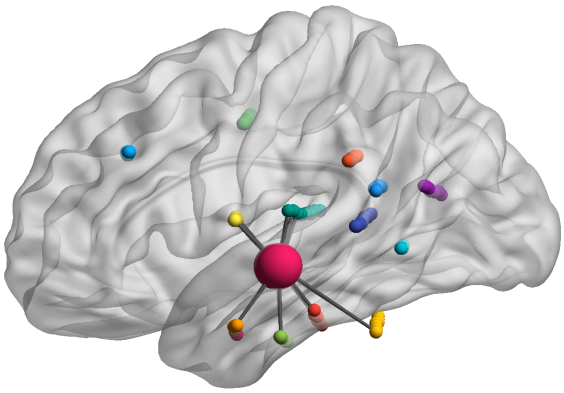

Fig. 5: Predicted Spread network of Patient 1: the large red node is the seizure onset area, and the connected nodes to the large red node are the predicted cortical sites that should receive seizure attack from the origin sites.

problem into a classical supervised sparse representation problem, which there exist a plenty of algorithms to solve. The proposed framework achieved satisfactory result.

Through CCEP mapping, we can develop new network generation scheme and scalable efficient algorithms for directed brain connectivity analysis. The scope of this study is planned as a step forward to understand neural circuits of epilepsy and provide a new computational framework to understand seizure focus, initiating seizure circuits, paths of spread, neuromodulatory centers, and to develop a system's view of epilepsy. It will establish valuable knowledge of seizure-spread networks and their relationship with some critical factors in presurgery assessment. The brain network analysis methods can also be generalized to analyze other brain disorders or cognitive functions of the brain with immediate clinical implications. In our future research, the sensitivity and specificity error rate will also taking into account in the goal function formulation instead of the overall accuracy as we studied here.

References

1. Barabási, A.L., Albert, R.: Emergence of scaling in random networks. science 286(5439), 509–512 (1999)
2. Bullmore, E., Sporns, O.: Complex brain networks: graph theoretical analysis of structural and functional systems. Nature Reviews Neuroscience 10(3), 186–198 (2009)
3. Deco, G., Tononi, G., Boly, M., Kringelbach, M.L.: Rethinking segregation and integration: contributions of whole-brain modelling. Nature Reviews Neuroscience 16(7), 430–439 (2015)
4. Delorme, A., Makeig, S.: Eeglab: an open source toolbox for analysis of single-trial eeg dynamics including independent component analysis. Journal of Neuroscience Methods 134(1), 9 – 21 (2004)
5. Donoho, D.L., Tsaig, Y.: Fast solution of-norm minimization problems when the solution may be sparse. Information Theory, IEEE Transactions on 54(11), 4789–4812 (2008)
6. Enatsu, R., Piao, Z., OConnor, T., Horning, K., Mosher, J., Burgess, R., Bingaman, W., Nair, D.: Cortical excitability varies upon ictal onset patterns in neocortical epilepsy: a cortico-cortical evoked potential study. Clinical Neurophysiology 123(2), 252–260 (2012)
7. Friston, K.J.: Functional and effective connectivity: a review. Brain connectivity 1(1), 13–36 (2011)

8. Guan, Z.H., Liu, F., Li, J., Wang, Y.W.: Chaotification of complex networks with impulsive control. Chaos: An Interdisciplinary Journal of Nonlinear Science 22(2), 023137 (2012)
9. Jefferys, J.G.: Basic mechanisms of epilepsy. Epilepsia (2009)
10. Jefferys, J.G.: Advances in understanding basic mechanisms of epilepsy and seizures. Seizure 19(10), 638 – 646 (2010)
11. Keller, C.J., Honey, C.J., Entz, L., Bickel, S., Groppe, D.M., Toth, E., Ulbert, I., Lado, F.A., Mehta, A.D.: Corticocortical evoked potentials reveal projectors and integrators in human brain networks. The Journal of Neuroscience 34(27), 9152–9163 (2014)
12. Keller, C.J., Honey, C.J., Mégevand, P., Entz, L., Ulbert, I., Mehta, A.D.: Mapping human brain networks with cortico-cortical evoked potentials. Phil. Trans. R. Soc. B 369(1653), 20130528 (2014)
13. Kim, D.W., Kim, H.K., Lee, S.K., Chu, K., Chung, C.K.: Extent of neocortical resection and surgical outcome of epilepsy: intracranial eeg analysis. Epilepsia 51(6)
14. Kreuz, T.: Measures of neuronal signal synchrony 6(12), 11922 (2011), revision 152249
15. Lega, B., Dionisio, S., Flanigan, P., Bingaman, W., Najm, I., Nair, D., Gonzalez-Martinez, J.: Cortico-cortical evoked potentials for sites of early versus late seizure spread in stereoelectroencephalography. Epilepsy research 115, 17–29 (2015)
16. Letzen, J.E., Craggs, J.G., Perlstein, W.M., Price, D.D., Robinson, M.E.: Functional connectivity of the default mode network and its association with pain networks in irritable bowel patients assessed via lidocaine treatment. The Journal of Pain 14(10), 1077–1087 (2013)
17. Liu, J., Ji, S., Ye, J., et al.: Slep: Sparse learning with efficient projections. Arizona State University 6, 491 (2009)
18. Nathan, S.S., Sinha, S.R., Gordon, B., Lesser, R.P., Thakor, N.V.: Determination of current density distributions generated by electrical stimulation of the human cerebral cortex. Electroencephalography and clinical neurophysiology 86(3), 183–192 (1993)
19. Newman, M.E.: The structure and function of complex networks. SIAM review 45(2), 167–256 (2003)
20. Otti, A., Guendel, H., Henningsen, P., Zimmer, C., Noll-Hussong, M.: Functional network connectivity of pain-related resting state networks in somatoform pain disorder: an exploratory fmri study. Journal of psychiatry & neuroscience: JPN 38(1), 57 (2013)
21. Sporns, O.: Structure and function of complex brain networks. Dialogues Clin Neurosci 15(3), 247–262 (2013)
22. Sporns, O., Tononi, G., Kötter, R.: The human connectome: a structural description of the human brain. PLoS Comput Biol 1(4), e42 (2005)
23. Uddin, L.Q., Clare Kelly, A., Biswal, B.B., Xavier Castellanos, F., Milham, M.P.: Functional connectivity of default mode network components: correlation, anticorrelation, and causality. Human brain mapping 30(2), 625–637 (2009)
24. Vecchio, F., Miraglia, F., Curcio, G., Della Marca, G., Vollono, C., Mazzucchi, E., Bramanti, P., Rossini, P.M.: Cortical connectivity in fronto-temporal focal epilepsy from eeg analysis: a study via graph theory. Clinical Neurophysiology 126(6), 1108–1116 (2015)
25. Wang, H., Fan, W., Yu, P.S., Han, J.: Mining concept-drifting data streams using ensemble classifiers. In: Proceedings of the ninth ACM SIGKDD international conference on Knowledge discovery and data mining. pp. 226–235. ACM (2003)
26. Watts, D.J., Strogatz, S.H.: Collective dynamics of small-worldnetworks. nature 393(6684), 440–442 (1998)
27. Wright, S.J., Nowak, R.D., Figueiredo, M.A.: Sparse reconstruction by separable approximation. Signal Processing, IEEE Transactions on 57(7), 2479–2493 (2009)
28. Yaffe, R.B., Borger, P., Megevand, P., Groppe, D.M., Kramer, M.A., Chu, C.J., Santaniello, S., Meisel, C., Mehta, A.D., Sarma, S.V.: Physiology of functional and effective networks in epilepsy. Clinical Neurophysiology 126(2), 227–236 (2015)
29. Ye, J., Liu, J.: Sparse methods for biomedical data. ACM SIGKDD Explorations Newsletter 14(1), 4–15 (2012)
30. Zhou, J., Seeley, W.W.: Network dysfunction in alzheimers disease and frontotemporal dementia: implications for psychiatry. Biological psychiatry 75(7), 565–573 (2014)